Towards non-classical light storage via atomic-vapor Raman scattering

C. H. van der Wal[a,b], M. D. Eisaman[a], A. S. Zibrov[a,b,c], A. André[a], D. F. Phillips[b], R. L. Walsworth[b], and M. D. Lukin[a]

[a]Department of Physics, Harvard University, Cambridge, MA, 02138, USA
[b]Harvard-Smithsonian Center for Astrophysics, Cambridge, MA, 02138, USA
[c]P. N. Lebedev Institute of Physics, RAS, Leninsky pr. 53, Moscow, 117924, Russia

ABSTRACT

We present experimental work that investigates whether quantum information carried by light can be stored via reversible mapping of the quantum state of such light onto a collective atomic coherence. Such a quantum memory could be utilized to allow quantum communication over long, lossy channels. Current efforts concentrate on writing a photon-number-squeezed state of light onto a collective coherence between the ground-state hyperfine levels of ^{87}Rb atoms in a warm vapor cell, and subsequent on-demand retrieval of this light. In this approach, intensity squeezing between the written and retrieved photon fields provides evidence for storage of a photon-number-squeezed state of light. The scheme is based on spontaneous Raman transitions that create the atomic coherence, and at the same time convert control fields into signal fields that propagate under conditions of electromagnetically induced transparency. We present experimental results demonstrating the storage and retrieval of light using this method, and discuss techniques for measuring intensity squeezing between these photon fields.

Keywords: Raman scattering, Squeezing, Light storage, Quantum communication, Quantum memory

1. INTRODUCTION

The experimental realization of long-distance quantum communication is of much interest, as it would allow secure transmission of messages and faithful transfer of unknown quantum states. Photons are very promising as carriers of quantum information over long-distances because their interaction with matter in the communication channel can be made very weak. Nevertheless, due to losses and decoherence, quantum communication fidelity decreases exponentially with channel length. This problem can be overcome by the use of entanglement purification protocols (quantum repeaters). However, since the purification protocols are probabilistic, some form of quantum memory is required to ensure polynomial scaling of the communication efficiency. Since it is difficult to store photons for long times, one approach to a practical quantum memory is to reversibly transfer the quantum information carried by photons into a non-photonic form. Duan *et al.*[1] propose using dense ensembles of resonant atoms as the medium for such a quantum memory as part of a quantum repeater-based implementation of long-distance quantum communication. The scheme is robust against significant storage and channel losses, non-ideal properties of photo-detectors, and the demand for resources grows only polynomially with increasing distance. The main challenge for implementing this proposal is that it requires the ability to store non-classical states of light, which has yet to be experimentally demonstrated. Storage of classical light pulses has been demonstrated in atomic ensembles[2,3] using a dynamic form of electromagnetically induced transparency[4] (EIT). The phase coherence of this process has also been demonstrated, as well as the ability to control the phase of the released light through straightforward manipulation of the collective excitation stored in the atomic ensemble.[5]

In this manuscript we present experimental work that investigates whether quantum information carried by non-classical light can be stored using an ensemble of ^{87}Rb atoms as the quantum memory medium. After a short introduction to the general ideas and preliminary experimental results, the main part of the manuscript addresses the question how the storage of non-classical light can be demonstrated in the presence of losses,

Further author information: (Send correspondence to C.H.W.)
C.H.W.: E-mail: cwal@cfa.harvard.edu, Telephone: 1 617 495 4177

Noise and Information in Nanoelectronics, Sensors, and Standards, L. B. Kish, F. Green, G. Iannaccone, J. R. Vig, Editors, Proceedings of SPIE Vol. 5115 (2003) © 2003 SPIE · 0277-786X/03/$15.00

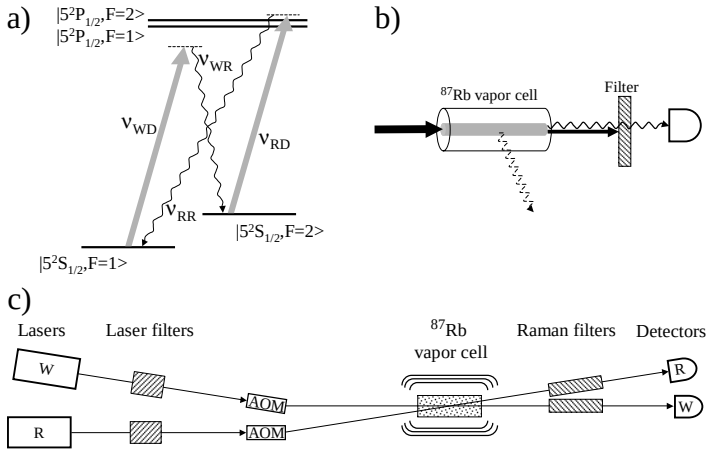

Figure 1. a) ^{87}Rb levels used in the light-storage experiments (D_1 line, the Zeeman sublevels are not shown in this simplified scheme, the ground-state hyperfine splitting is 6.835 GHz). With optical pumping the atoms are prepared in the $|5^2S_{1/2}, F = 1\rangle$ state. The Write step is a spontaneous Raman transition induced with a drive field at optical frequency ν_{WD}, and Raman signal field at optical frequency ν_{WR}. This process creates a small population in the $|5^2S_{1/2}, F = 2\rangle$ state with a coherence between $|5^2S_{1/2}, F = 1\rangle$ and $|5^2S_{1/2}, F = 2\rangle$. In the Read step this coherence is mapped back into an optical field ν_{RR} with a second Raman transition induced with a drive field ν_{RD}. **b)** Collective enhancement of spontaneous Raman light. The beam volume of the drive field (solid black) forms a pencil-shaped volume (gray) in the vapor cell with high gain for spontaneous Raman fields. Spontaneous Raman fields are weakly emitted in all directions (wiggly dashed), but are strongly enhanced in the direction co-propagating with the drive field (wiggly solid). As a result, almost all spontaneous Raman light is detected in a setup with a detector aligned with the drive field and a filter that blocks the transmitted drive field. **c)** Schematic of the experimental setup. Two lasers provide the Write (W) and Read (R) drive fields, with acousto-optic pulse modulation (AOM). The beam volumes of the two drive fields overlap in the Rb vapor cell. A small angle (smaller than in this schematic representation) between the drive beams allows for spatially separated detection of the co-propagating Write and Read Raman fields. The vapor cell is placed in an oven inside three layers of magnetic shielding. Filters after the lasers are used to suppress the spontaneous emission background and spurious modes. Filters before the detectors block the transmitted drive fields such that only the Raman fields are detected.

and delays from EIT effects in the atomic medium. The current experiments aim at writing a photon-number-squeezed state of light onto a collective coherence between the ground-state hyperfine levels of ^{87}Rb atoms in a warm vapor, and subsequent retrieval of squeezed light after a controllable storage time. The current scheme relies on a spontaneous Raman transition combined with photon-number measurement of the Raman light for the creation of the squeezed atomic coherence. For retrieval, a second Raman process is used for converting this atomic excitation into squeezed light. It is predicted that successful storage of such non-classical states should result in intensity squeezing between the stored and retrieved light. We describe our experimental methods and progress towards observing such squeezing in the presence of unbalanced losses and delays between the stored and retrieved light.

An outline of the text is as follows. In section 2 we summarize the ideas regarding the storage of non-classical light in atomic ensembles. In section 3 we describe preliminary results of the experimental implementation of these ideas. A full account of these experimental results will be published elsewhere, and the presentation here mainly serves as an illustration for the main part of the manuscript in section 4. In section 4, we present experimental techniques that are needed for investigating twin-mode intensity squeezing.

2. STORAGE OF NUMBER-SQUEEZED LIGHT IN ATOMIC ENSEMBLES

The proposal by Duan *et al.*[1] for setting up long-distance entanglement requires storage of photon-number squeezed states of light. We will summarize here those parts of the proposal that are relevant for the remainder of this manuscript, and assume that ensembles of ^{87}Rb atoms are used for storage.

Light storage in atomic ensembles is based on electromagnetically induced transparency (EIT).[4,6,7] It requires an ensemble of atomic Λ-systems with two low-energy states $|g\rangle$ and $|s\rangle$, and an excited state $|e\rangle$ (similar to Fig. 1a). A strong control field drives the $|s\rangle$-$|e\rangle$ transition, and a weak signal field is tuned to the $|g\rangle$-$|e\rangle$ transition in such a way that the two fields are two-photon resonant for the $|g\rangle$-$|s\rangle$ transition. Under these conditions the signal field propagates in the atomic ensemble as a dressed field-atom quasiparticle, a so-called dark-state polariton.[8,9] The group velocity of this dark-state polariton is proportional to the intensity of the control field. If the control field is adiabatically reduced to zero when a signal pulse is in the atomic ensemble, then the group velocity of the signal pulse will be reduced to zero and the dark-state polariton will become purely atomic. The properties of the signal light pulse are thus mapped onto a collective coherence of atomic spin states. Switching the control field back on reverses this storage process: the signal group velocity and the photonic part of the dark-state polariton are restored, and the signal field propagates as it did before storage. This light storage technique has been verified qualitatively using classical light pulses and warm ^{87}Rb vapor.[3,5]

In principle the storage of non-classical light can be a straightforward extension of the above technique with a signal pulse that comes from a non-classical source of light. Alternatively, a state that is equal to the storage of a photon-number squeezed state of light can be prepared in an atomic vapor in a probabilistic manner using spontaneous Raman transitions and a measurement to project the atomic light-storage state onto a number state. This latter approach, employed in our current experiments (and known as the *Write* step), has the advantage that one can work without a non-classical source of light.

With optical pumping the atoms are first prepared in the $|g\rangle = |5^2\mathrm{S}_{1/2}, \mathrm{F} = 1\rangle$ state. As illustrated in Fig. 1a, for a ^{87}Rb ensemble driven near its D_1 transition, a pulse of drive field at optical frequency ν_{WD} induces a spontaneous Raman (Stokes) transition, and a Raman signal field at optical frequency ν_{WR} propagates in the ensemble under EIT conditions. This process creates a small population in the $|s\rangle = |5^2\mathrm{S}_{1/2}, \mathrm{F} = 2\rangle$ state with a collective coherence between $|5^2\mathrm{S}_{1/2}, \mathrm{F} = 1\rangle$ and $|5^2\mathrm{S}_{1/2}, \mathrm{F} = 2\rangle$. That is, the Raman scattering is uniquely correlated with the excitation of a collective atomic spin wave mode $\hat{S}$ that is a symmetric superposition $\hat{S} = (1/\sqrt{N_a}) \sum |g\rangle\langle s|$, where the summation is over all N_a atoms in the ensemble. Before the Raman transition, the Raman mode at optical frequency ν_{WR} and the atomic spin wave S are in the vacuum state $|0\rangle_{phot} \otimes |0\rangle_{spin}$. The Raman transition is a spontaneous (i.e., initiated by vacuum fluctuations) but coherent process in which the classical drive field induces coherent evolution from the vacuum state $|0\rangle_{phot} \otimes |0\rangle_{spin}$ to a superposition of number states[10,11]

$$|\Psi\rangle = \sum_{n=0}^{\infty} c_n |n\rangle_{phot} \otimes |n\rangle_{spin} \,. \tag{1}$$

The probability amplitudes c_n have a thermal distribution[12,13] $c_n = \overline{n}^n/(\overline{n}+1)^{n+1}$, where $\overline{n}$ is the expectation value for the number of photons in the signal Raman mode. This Raman field and the spin wave form a coherent superposition with entanglement between the (ideally equal) number of photons and number of collective spin excitation quanta. Subsequent measurement of the intensity (or photon number) of the Raman Stokes field is destructive for the photonic part of (1), but projects the spin part onto a particular number state and thus leaves the atomic ensemble in a state equal to the storage of a photon-number state of light (Fock state).

In a subsequent *Read* step the spin wave number state $|n\rangle_{spin}$ is mapped back onto a second optical Raman field. The physical mechanism for this step is identical to the retrieval of weak classical pulses in recent light-storage experiments.[2,3,5] This Read Raman process is stimulated by the atomic coherence. A drive field at frequency ν_{RD} induces a Raman transition that returns the entire ^{87}Rb population to the initial state and creates a Raman (anti-Stokes) field with a number of photons equal to that measured in the Write step. Hence, measurement of the number of photons in this anti-Stokes field should show very strong correlations with the number of photons measured in the Stokes field (twin-mode intensity squeezing). Also note that this process provides a probabilistic photonic Fock-state-on-demand source.

In the discussion so far we have neglected the question of whether all the Raman fields can be efficiently measured in a single detection process. In principle, spontaneous Raman fields are emitted in all directions; nevertheless, collective emission from atomic ensembles can be highly directional due to collective enhancement[1] (Fig. 1b). The atomic ensemble is prepared in the $|5^2S_{1/2}, F = 1\rangle$ state, which acts like a population inversion with corresponding gain for the spontaneous Write field. This gain is only manifest in the beam volume of the drive field for the Write step. For long pencil-shaped beam volumes with N_a atoms, there is thus highly directional gain for the spontaneous Write field, which gives a $\sqrt{N_a}$ enhancement for the spontaneous Raman scattering rate in the direction of the drive field.[1] Therefore, effectively all Raman emission co-propagates with the drive beam, which allows for efficient detection of the Raman fields. An additional important technical issue, phase matching of the optical fields, is discussed in Ref. 14, but is easily fulfilled with our atomic-vapor ensembles.

3. PRELIMINARY EXPERIMENTAL RESULTS

In this section we present preliminary observations of the phenomena discussed in the previous section. To date, we have observed highly correlated modes of spontaneous Write Raman light and retrieved Read Raman light that are predominantly emitted in the direction co-propagating with the drive fields (collective enhancement).

The scheme used for these experiments is shown in Fig. 1c. A warm ^{87}Rb vapor cell with a length of 7 cm is maintained at a temperature of typically $\approx$ 80 °C, corresponding to an atom number density of $\approx 10^{12}$ cm^{-3}. Two extended-cavity diode lasers provide the Write and Read drive fields. The drive fields have typical powers of a few mW, and are focused in the cell to diameters of about 0.5 mm. The time scale for atoms moving out of the beam volume is made longer with a Ne buffer gas of 3 torr (giving diffusion times in the μs to ms range). We observed spontaneous Raman signals for both linear and circular polarizations of the drive fields, and at several detunings, typically about 1 GHz from 1-photon resonance on the ^{87}Rb D_1 transition (see Fig. 1 a). The Read drive laser or a third laser was used for optical pumping. We employed filters (based on diffraction gratings) following each laser to suppress the spontaneous emission background and spurious modes of the lasers in the drive fields. The drive fields can be modulated with acousto-optic modulators. The beam volumes of the two drive fields overlap in the Rb cell, and a small angle ($\approx$ 3 mrad) between the drive beams allows for spatially separated detection of the Write and Read Raman fields that co-propagate with the drive fields. Filters following the vapor cell (for different experimental circumstances, we used filters based on ^{85}Rb atomic absorption cells, Fabry-Perot etalons or polarizing beam splitters) block the transmitted drive fields such that only Raman fields reach the detectors. Scanning Fabry-Perot etalons and beatnote detection of Raman fields in the presence of transmitted drive fields (i.e., without downstream filters) were used for identifying the Raman modes.

Figure 2 presents examples of synchronously detected Raman signals at optical frequencies ν_{WR} and ν_{RR} (see Fig. 1a) in modes that co-propagate with the drive fields. We only observed detectable levels of Raman fields in narrow conical volumes around the transmitted drive beams, which indicates that collectively enhanced emission is dominant for our Raman signals. The Raman transitions were induced with continuous-wave (CW) drive fields, and the Raman signals can be thought of as the result of a four-wave mixing process.[14] By large detuning of the Write drive field, the associated Raman transition is the bottleneck in the CW four-wave mixing, and the current experiment can be interpreted as a CW version of the light storage mechanism described in the previous section.

The Write transition is a spontaneous process that gives thermal photon statistics to the Write Raman field and thus leads to strong fluctuations in the intensity of the observed Write Raman signal.[10] The bandwidth of these fluctuations is limited by the collective Raman transition rate in the Write step. Giving the Read drive a higher intensity and smaller detuning than the Write drive leads to a faster and more efficient Read Raman transitions. Under these conditions, and with CW drive fields, the Read field rapidly converts the spin wave that results from Write Raman transitions into a dark-state polariton. Also, the collective enhancement of this process leads to the combined propagation of Write and Read Raman fields under EIT conditions.[15] The bandwidth of this combined Raman process is $\Delta_R = \Omega_W \Omega_R / \Delta$, where the Ω_i are the Rabi frequencies of the drive fields and Δ is the Write drive detuning, and the fluctuations in the Read Raman field are predicted to be delayed with respect to the Write field fluctuations by $\Delta t \approx 1/\Delta_R$.[15] In practice in the current experiment the bandwidth of this Raman process is narrower than the EIT transparency bandwidth for the signal fields.

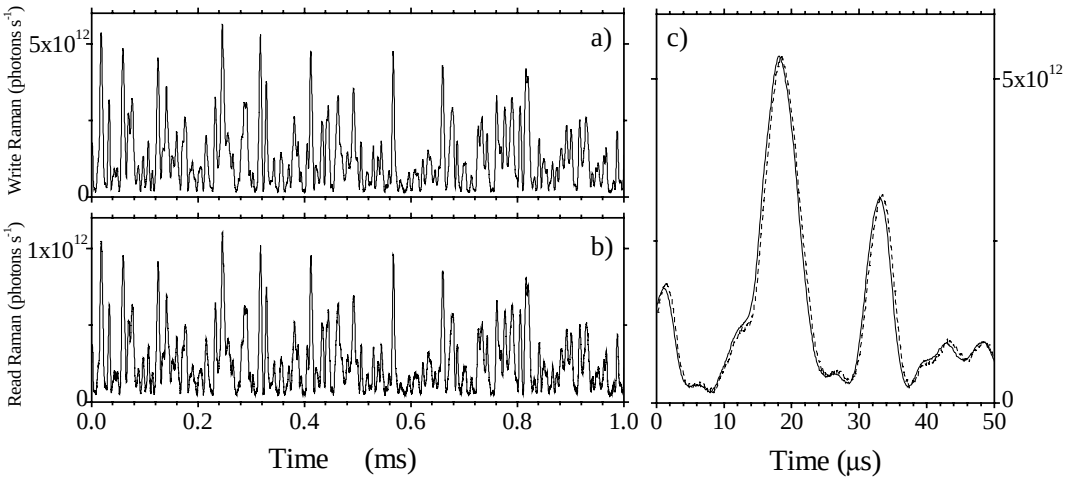

Figure 2. Examples of synchronously detected Raman signals from the spontaneous Write mode **(a)** and retrieved Read mode **(b)** showing strong correlations (plotted here for an effective sampling time of 100 ns, note the different vertical scale). The Raman transitions are induced with CW drive fields, under conditions where the Write transition is the bottleneck for the four-wave mixing scheme of Fig. 1a. The noisy nature of the signals results from the thermal photon statistics of the spontaneous Write mode. The bandwidth of the fluctuations is limited by the Raman process (not by the detection bandwidth). **c)** The first 50 μs of the traces in a) and b). The Write trace (solid) is plotted as in a), the Read trace (dashed) is multiplied by 5.167 and given a small offset (to correct for a weak constant background signal from the drive field leaking through the filter) to match the Write trace. Plotted on this scale one can observe small differences between the two traces and a delay for the Read signal (here 292 ns), due to slow-light EIT effects.

Note that the Write and Read Raman fields in this process are correlated at the quantum level, since the creation of the Raman fields is always accompanied by an atomic spin flip. Hence, there should be strong correlations between the observed Write and Read signals. However, we have found that the photon numbers in the Write and Read mode are not equal. While our observations show the relative fluctuations in each mode to be very similar (Figs. 2a and 2b), the Read mode is about 5 times weaker than the Write mode (Fig. 2c). The mechanism responsible for the attenuated Read signal is not yet fully understood. We have determined experimentally that part of the Read signal attenuation is due to imperfect spatial mode matching of the Write and Read drive fields; we have also found that for Raman signals as in Fig. 2, the Read process is drive-power limited. In addition, Fig. 2c shows that the Read signal follows the Write signal with a short delay. This delay is the result of the slow-light EIT effects discussed above.[15] In section 4 we will discuss how one can investigate twin-mode intensity correlations between Raman signals with such unbalanced attenuations and delays.

Figure 3 presents Raman signals recorded under similar conditions to the CW experiment of Fig. 2, but instead using pulsed drive fields. Here also the intensity of the Write Raman signal shows strong fluctuations in sequential repetitions, with correlated fluctuations in the intensity of the Read Raman pulses. This pulsed experiment realizes the storage of spontaneous Raman light on hyperfine levels, similar to the techniques in the proposal of Duan *et al.*[1] Here, the Write and Read drive pulses do not overlap temporarily, and switching on the Read drive at later times results in a correspondingly delayed Read Raman pulse, with a fall-off in intensity that is in reasonable agreement with diffusive losses of atoms from the beam volume. The pulsed drive data presented here shows a Read/Write efficiency of about 1/50. In recent experiments we have found this inefficiency arises from limitations similar to those of the CW experiment discussed above; very recently, the efficiency has been improved.

Further indications that this pulsed experiment is a realization of light storage come from the following tests. Upon removing the Write drive pulse both the Write and Read Raman signals vanish. Removing the Read drive

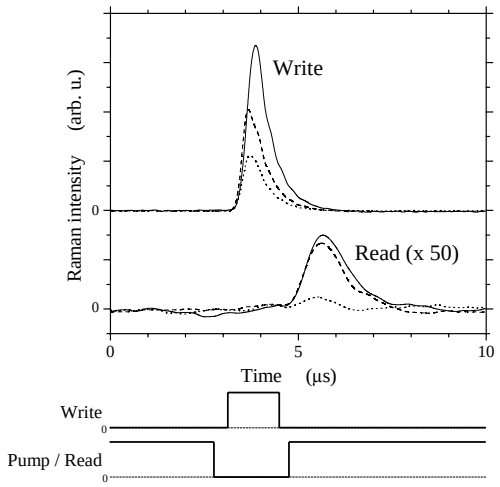

Figure 3. Demonstration of light storage on hyperfine levels with spontaneous Raman Write and retrieved Read signals and pulsed drive fields. The Read drive field is first used for optical pumping, followed by non-overlapping Write and Read drive pulses which create and retrieve Raman Write and Read signals. The traces below the data plot represent the modulation of the control fields. Consecutive realizations of the experiment (solid, dashed, dotted) show strong fluctuations in the Write pulse intensity, and correlated fluctuations in the Read pulse intensity. (Background signals from drive fields leaking through the filters are subtracted; pulse shapes are limited by the detection bandwidth.)

after the Write pulse showed results with only Write Raman signals. Removing optical pumping before the Write pulse gave no detectable levels of Raman Write or Read signals; we conclude that the observed Raman signals result from collective enhancement (removing the optical pumping stage takes away the gain for the spontaneous Write Raman field). Furthermore, all Raman light was observed in a narrow conical volume around the transmitted drive beams.

4. TWIN-MODE SQUEEZING WITH UNBALANCED LOSSES AND DELAYS

4.1. Introduction

When the number of photons in two modes of light are measured in a repetitive manner (with paired results n_1 and n_2), the general criterion for correlations (here termed classical correlations) between n_1 and n_2 is

$$\mathrm{Var}(n_1 - n_2) < \mathrm{Var}(n_1) + \mathrm{Var}(n_2)\,. \tag{2}$$

Here Var is used as notation for the variance in a set of measurements. A repetitive measurement on a single classical mode of light with average photon number $\overline{n}$ yields a variance $\mathrm{Var}(n) \geqq \overline{n}$, due to quantum fluctuations of at least $\sqrt{\overline{n}}$ in the photon number of the mode. The case $\mathrm{Var}(n) = \overline{n}$ holds for a coherent state, which has Poissonian photon statistics, and is referred to as the standard quantum limit of noise.[12,13] Accordingly, one can define that two modes of light have non-classical correlations when for paired measurements n_1 and n_2

$$\mathrm{Var}(n_1 - n_2) < \overline{n}_1 + \overline{n}_2\,, \tag{3}$$

and meeting this criterion is known as twin-mode intensity squeezing.[16] Note that for propagating modes of light the relevant photon number is set by $n = \Phi_n/R$, where Φ_n is the photon flux and R is the detection sample rate.

The two Raman fields in light-storage experiments as presented in the previous sections are predicted to show such twin-mode intensity squeezing. However, to date, due to to losses and inefficiencies in the Read process, the measured values $\overline{n}_1 \neq \overline{n}_2$ (Fig. 2). While this inefficiency can probably be improved, in many future experiments

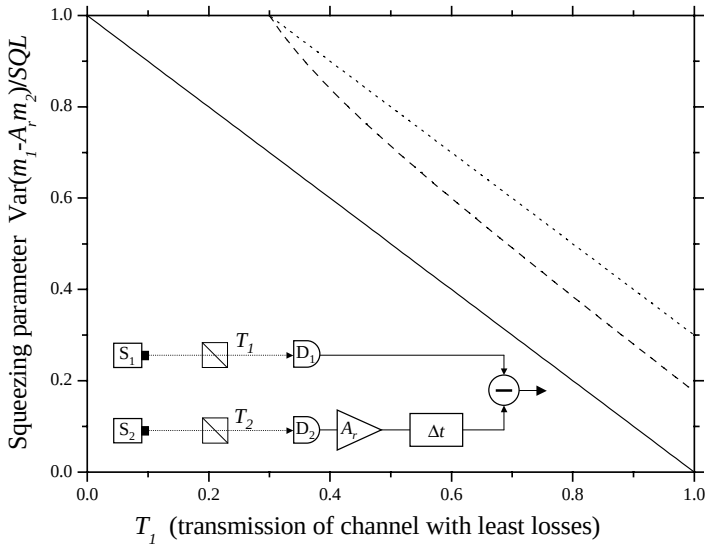

Figure 4. Inset: Model used for investigating twin-mode intensity squeezing in the presence of unbalanced losses and delays (see text for details). **Main graph:** Twin-mode intensity squeezing parameter $SQP = \mathrm{Var}(m_1 - A_r m_2)/SQL$, with $SQL = \overline{m}_1 + A_r^2 \overline{m}_2$, for the two modes detected in the model of the inset. The solid line is for $T_2 = T_1$ and $A_r = 1$. The dotted line is for $T_2 = T_1 - 0.3$, and compensating the difference between T_1 and $A_r T_2$ by inserting additional losses into channel 1 and keeping $A_r = 1$ (i.e., $T_1' = T_2$). The dashed line is for $T_2 = T_1 - 0.3$, and compensating the difference between T_1 and $A_r T_2$ with a noise-free amplification factor $A_r = T_1/T_2$.

losses and other imperfections will remain and cause significant differences between observed values of $\overline{n}_1$ and $\overline{n}_2$ in experiments where they are in principle equal. Furthermore, spontaneous Raman modes have thermal photon statistics (i.e., large excess noise[12,13] with $\mathrm{Var}(n) = \overline{n} + \overline{n}^2$). As a result, $\mathrm{Var}(n_1 - n_2)$ will be very large for data sets with $\overline{n}_1 \neq \overline{n}_2$. A second problem that hampers a test for twin-mode intensity squeezing is a delay between the detection of correlated pairs n_1 and and n_2 (Fig. 2c). Subtraction of measured values n_1 and n_2 without compensation for this delay will also lead to increased values for $\mathrm{Var}(n_1 - n_2)$.

The question that we will address in section 4.2 is how tests for twin-mode intensity squeezing can be performed in experiments with significant unbalanced losses and delays between the two Raman modes. In section 4.3 we will discuss requirements for the detection systems for such research.

4.2. Tests for twin-mode squeezing with unbalanced losses and delays

Fig. 2c illustrates that the residual signal $(n_1 - n_2)$ is strongly reduced by multiplying the Read Raman data set by a relative compensation factor A_r. Accordingly, the variance of $\mathrm{Var}(n_1 - A_r n_2)$ is reduced as well. This compensation can be carried out without adding noise, because it can be implemented as a simple multiplication of photon-count results. Alternatively, the measured values of n_1 and n_2 can be made equal by inserting additional losses into the stronger mode before detection. However, such optical attenuation will introduce additional noise. When implementing such strategies for reducing $\mathrm{Var}(n_1 - n_2)$, one needs to reexamine the definition and meaning of twin-mode intensity squeezing in Eq. (3). This will be analyzed below.

For this analysis we will assume a simple model shown in the inset of Fig. 4. Two sources S_1 and S_2 send out Fock states with photon numbers n_1 and n_2. The values for n_1 and n_2 fluctuate, but are perfectly correlated in pairs with $n_1 = n_2$. However, the emission from S_1 is delayed by Δt, with Δt larger than the emission repetition rate. The photon number in the emitted modes are detected at this repetition rate with photon counters D_1 and D_2. Losses in the channels between the sources and detectors are modeled with beam splitters with transmission T_1 and T_2, and we will assume $T_1 \geqq T_2$. Due to the losses, the measured photon numbers will be smaller than

what is emitted, and the photon-count results will be denoted as m_1 and m_2. The detectors are assumed to be perfect (no dark counts, and imperfect detection efficiencies are included in T_1 and T_2). The detectors report photon number per event. Before subtraction and comparison to Equation (3), the count results in channel 2 can be multiplied by a noise-free relative amplification factor A_r, and delayed by Δt.

When the paired fluctuations in n_1 and n_2 are large and $T_1 \neq T_2$, the variance in the subtracted signal $\mathrm{Var}(m_1 - m_2)$ will be large as well. In this case, the value $\mathrm{Var}(m_1 - m_2)$ is not representative for the fundamental correlations between the signals, but a trivial artifact of the unequal losses in the two channels. As mentioned before, this can be dealt with by inserting additional losses into channel 1 to give $T_1' = T_2$ or by amplifying the results of channel 2 with $A_r = T_1/T_2 = \overline{m}_1/\overline{m}_2$. More generally, one needs to realize $T_1 = ArT_2$. This suggests that one can replace the condition for twin-mode intensity squeezing (Eq. (3)) with

$$\mathrm{Var}(m_1 - A_r m_2) < \overline{m}_1 + A_r^2 \overline{m}_2 \,, \tag{4}$$

assuming that one has set

$$A_r = \overline{m}_1/\overline{m}_2 \,. \tag{5}$$

The right hand side of (4) is the adjusted level for the standard quantum limit, $SQL = \overline{m}_1 + A_r^2\overline{m}_2$. The factor A_r^2 needs to be introduced because (4) compares the fluctuations of a mode to the fluctuations of a coherent state, and these are amplified in our model as well. Below we will analyze four cases where this new definition for squeezing is used (see also Fig. 4). We will calculate the squeezing parameter SQP, defined as

$$SQP = \frac{\mathrm{Var}(m_1 - A_r m_2)}{\overline{m}_1 + A_r^2\overline{m}_2} = \frac{\mathrm{Var}(m_1 - A_r m_2)}{SQL} \,, \tag{6}$$

which is smaller than 1 in case of twin-mode squeezing, and equal to 0 for perfect twin-mode squeezing.

i) $T_1 = T_2$ *and* $A_r = 1$: The beam splitters, with equal transmission, randomly remove photons from the modes, and this process gives partition noise in m_i, with , for fixed n_i, a binomial variance $\mathrm{Var}(m_i) = n_i T_i(1-T_i)$, $i = 1,2$, see Refs. 12,13. This leads to the familiar result $SQP = (n_1T_1(1-T_1) + n_2T_2(1-T_2))/(n_1T_1 + n_2T_2) = 1 - T_1$. Averaging over fluctuations in n_i does not alter the result. Squeezing can still be observed, but the value for SQP approaches 1 for significant losses. See the solid line in Fig. 4.

ii) $T_1 > T_2$, *which is compensated by inserting additional losses into channel 1 to give* $T_1' = T_2$, $A_r = 1$: The analysis goes as for the previous case, but now the result is $SQP = 1 - T_2$. The squeezing parameter is set by the channel with the most losses. See the dotted line in Fig. 4.

iii) $T_1 > T_2$ *and* $A_r = T_1/T_2 = \overline{m}_1/\overline{m}_2$: Working it out as for case i) gives $SQP = (1 - T_1 + (T_1/T_2)(1 - T_2))/(1 + T_1/T_2)$. As compared to case ii) there is an improvement in the observable minimum SQP. See the dashed line in Fig. 4.

iv) $T_1 > T_2$ *and* $A_r = T_1/T_2 = \overline{m}_1/\overline{m}_2$, *but the sources* S_1 *and* S_2 *send out classical photon wave packets instead of Fock states*: For comparison, we will analyze SQP for the parameters of iii) for the situation where the sources S_1 and S_2 send out classical photon wave packets (coherent states, with uncorrelated quantum fluctuations) with photon-number expectation values $\overline{n}_1 = \overline{n}_2$. We consider the simplest case where $\overline{n}_1$ and $\overline{n}_2$ are constant in time. When a coherent state is attenuated its photon statistics remain Poissonian.[12,13] This gives $\overline{m}_i = T_i\overline{n}_i$ with $\mathrm{Var}(m_i) = \overline{m}_i$, and yields $SQP = 1$. This shows that $SQP < 1$ cannot be realized with very stable classical fields.

The above analysis shows that Equations (4)-(6) provide a valid test for twin-mode intensity squeezing useful in many realistic experimental situations. Squeezing is identified by values $SQP < 1$, and this cannot be realized with two classical fields (coherent states) with uncorrelated fluctuations. However, as usual, observation of significant squeezing (say $SQP < 0.5$, i.e., more than 3 dB squeezing) requires both $T_1 > 0.5$ and $T_2 > 0.5$.

4.3. Hardware requirements for detection of twin-mode squeezing

In the previous subsection we discussed the need for unbalanced losses and delays to be sufficiently compensated in order to observe twin-mode intensity squeezing. In this subsection we discuss the requirements on the detection hardware for implementing such experiments.

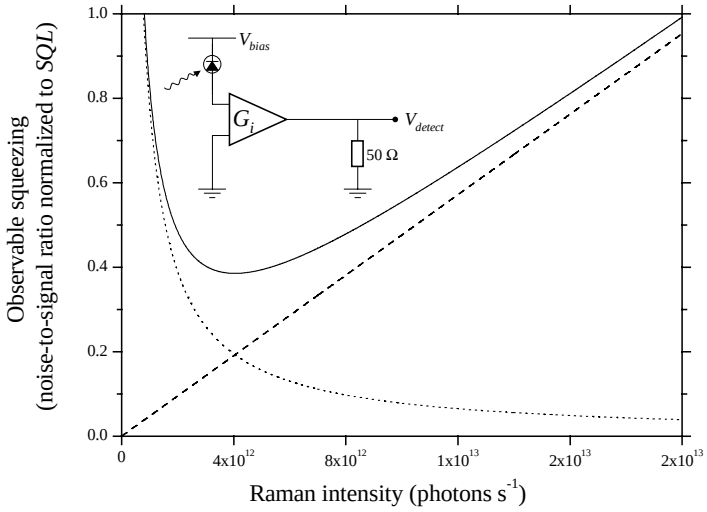

Figure 5. Inset: Generic photo-detector-amplifier circuit. The photo-current from a photo-diode (voltage biased in reverse at V_{bias}) is current-amplified with gain G_i, and voltage detected (V_{detect}) with 50 Ω technology. **Main graph:** Observable squeezing parameters $\mathrm{Var}(n)/\overline{n}$ for measurements on a Fock state with photon number $\overline{n}$, as limited by technical noise-to-signal ratios normalized to the fluctuation-to-signal ratio for the standard quantum limit $SQL = 1/\overline{n}$. The dotted line is for a white noise floor in the detection process (here plotted for current amplification $G_i = 5000$ and a white noise level of 50 $\mathrm{nV}/\sqrt{\mathrm{Hz}}$). The dashed line results from the finite resolution of analog-to-digital sampling (here from adjacent averaging of data sampled at 8 GHz with 8 bit resolution and using $M_{th} = 5$, see the text for details). The solid line gives the sum of the two noise contributions. For the ^{87}Rb D_1 line (795 nm), an optical power of 1 μW $\approx 4 \cdot 10^{12}$ photons s^{-1}, and is a typical value for the Raman modes in our experiments.

The experimental challenges for implementing a scheme such as that shown in Fig. 1c and Fig. 4 are different for the regime with few-photon-number and large-photon-number Raman signals. In the limit with Raman signals of a few photons, the main challenge is to realize the low-loss Raman filters in Fig. 1c, which are needed to block the drive fields that are orders of magnitude stronger while introducing little losses for the Raman signal fields. In this limit photon counters must be used for detection, and dark counts and in particular dead-time effects hamper the analysis of results. In the case of Raman signals with a large number of photons, regular photo-detectors must be used. Here the main challenge is to meet requirements for low noise levels and high detection resolution. The technical white noise in the detected signals due to, for example, Johnson noise must be small compared to fluctuations of the signal field at the level of the standard quantum limit, which favors working with large photon numbers. However, the resolution for processing the signals needs to be better than the standard quantum limit as well. For signals at the standard quantum limit with average photon number $\overline{n}$, the fluctuation-to-signal ratio scales as (in terms of variances) $1/\overline{n}$. Thus meeting the resolution requirements favors working with small photon numbers. Below we will discuss the large-photon number case. The amplitude and delay corrections A_r and Δt can be implemented in hardware electronics. Alternatively, the signals representing $m_1(t)$ and $m_2(t)$ can be recorded with high resolution, and the A_r and Δt compensation can be implemented in software. These two approaches are equivalent. We will concentrate here on the latter case, but the requirements for noise levels and resolution can be directly transposed to the hardware case.

As mentioned, the fluctuation-to-signal ratio for fields with noise at the standard quantum limit scales as $1/\overline{n}$ in terms of variances. We will analyze the noise-to-signal ratios for white noise, as well as the resolution requirements, and normalize them to the standard quantum limit (Fig. 5). The signal is a photon flux $\Phi_n(t)$ measured at sample rate R. This sets the level for $\overline{n} = \overline{\Phi}_n/R$, and the noise-to-signal ratio for the standard quantum limit:

$$NSR_Q = R/\overline{\Phi}_n \,. \tag{7}$$

We will assume that the power (photon flux) of the signal fields is measured by probing the voltage of a circuit as in Fig. 5. With standard commercial components one can realize photo-detector-amplifier circuits with current amplification of $G_i = 5000$, a bandwidth larger than 1 MHz, and a white noise level below $\sigma_{V1\mathrm{Hz}} = 50\,\mathrm{nV}/\sqrt{\mathrm{Hz}}$.[17] With one electron (e) of photo-current per photon, the voltage signal level is then $\overline{\Phi}_n e G_i Z_{50}$, where Z_{50} is the 50 Ω impedance of the detection system. The voltage noise level is $\sigma_V = \sigma_{V1\mathrm{Hz}}\sqrt{R/2}$. This gives for the normalized noise-to-signal level (for white noise from the detection system):

$$NSR_W/NSR_Q = \frac{1}{\overline{\Phi}_n}\frac{\sigma^2_{V1\mathrm{Hz}}}{2(eG_iZ_{50})^2}\,, \tag{8}$$

see also Fig. 5. Note that the expression is independent of the sample rate R. The white noise of the detection system clearly sets a minimum level of $\overline{\Phi}_n$ for which squeezing can be observed.

Recording the signals will typically be implemented with an analog-to-digital sampling process, which needs to be accurate enough to confirm noise-to-signal levels that are smaller than NSR_Q. Because the Raman signals show large excess noise, the detection system needs more dynamic range than for a signal with Poissonian photon statistics; hence, for this resolution analysis we will compare to a signal level $\overline{n} = M_{th}\overline{\Phi}_n/R$. The margin M_{th} needs to be about a factor of 5 for signals with thermal photon statistics. We assume a sampling process with a certain number of bits (bit) and sample time τ_s. Oversampling and averaging over results recorded during $1/R$ can be used to enhance the effective resolution with a factor $\sqrt{\tau_s R}$. The finite recording resolution leads then to noise on the recorded signal with a normalized noise-to-signal ratio:

$$NSR_R/NSR_Q = \overline{\Phi}_n\frac{M^2_{th}\tau_s}{(2^{bit})^2}\,. \tag{9}$$

Note that this expression is also independent of the sample rate. The expression reflects that with increasing photon flux the resolution requirement scales as the standard quantum limit $1/\overline{n}$. Thus the finite recording resolution sets an upper limit on $\overline{\Phi}_n$ for which squeezing can be observed. (Note that at very low values of $\overline{\Phi}_n$ the relative sampling resolution cannot be realized, and for $\overline{\Phi}_n$ approaching zero the dashed line in Fig. 5 should curve up; it can be described as a source of white noise.) As shown in Fig. 5 for realistic parameters, there is a $\overline{\Phi}_n$-window for values as in Fig. 2 in which a squeezing parameter below 0.5 can be observed. This analysis was in terms of the detection of a single channel, but generalizing it to the statistics of two subtracted channels does not alter the values in Fig. 5. The results of this analysis are independent of sample rate R, but one should note that twin-mode intensity squeezing is only expected for experiments with R commensurate with the Raman bandwidth or smaller (about 200 kHz for the data in Fig. 2).

The discussion so far has been concerned with a test for squeezing in the time domain. Problems arising from technical $1/f$ noise can be dealt with by performing the test for squeezing in the frequency domain. The Discrete Fourier Transform formalism (DFT) can be used for a straightforward transformation of the recorded time series m_1 and m_2 and the criteria for squeezing.

5. CONCLUSIONS

We have observed both CW and pulsed light storage on atomic hyperfine levels in a warm vapor cell via Raman scattering. We have observed strong correlations between the Write and Read Raman signals, and developed techniques for testing the presence of quantum correlations between these signals. To date, carrying out frequency-domain tests for CW data sets as in Fig. 2, with the methods presented in the previous sections, we have demonstrated 30 dB of classical correlations within the Raman bandwidth. We are currently analyzing and correcting experimental imperfections that prohibit a test for intensity squeezing between the two Raman signals. In general, demonstrating very high levels of squeezing is difficult with optical systems. We have developed techniques that should allow for at least 3 dB of intensity squeezing via atomic vapor Raman scattering. With pulsed drive fields, such light storage techniques are a promising avenue for research on photonic quantum memories.

ACKNOWLEDGMENTS

We are grateful to T. P. Zibrova, J. MacArthur and M. Hohensee for experimental help, and to P. R. Hemmer and A. Trifonov for useful discussions. This work is supported by programs of the NSF, DARPA and ONR. Partial support by NASA and the MIT-Harvard Center for Ultracold Atoms is also acknowledged. CHW acknowledges support from a fellowship through the Netherlands Organization for Scientific Research (NWO). MDE acknowledges support from a National Science Foundation Graduate Research Fellowship.

REFERENCES

1. L. M. Duan, M. D. Lukin, J. I. Cirac, and P. Zoller, *Nature* **414**, 413 (2001).
2. C. Liu, Z. Dutton, C. H. Behroozi, and L. V. Hau, *Nature* **409**, 490 (2001).
3. D. F. Phillips, M. Fleischhauer, A. Mair, R. L. Walsworth, and M. D. Lukin, *Phys. Rev. Lett.* **86**, 783 (2001).
4. M. D. Lukin and A. Imamoğlu, *Nature* **413**, 273 (2001).
5. A. Mair, J. Hager, D. F. Phillips, R. L. Walsworth, and M. D. Lukin, *Phys. Rev. A* **65**, 031802 (2002).
6. E. Arimondo, in *Progress in Optics*, ed. E. Wolf, North-Holland, Amsterdam, Vol. **35**, p. 259 (1996).
7. S. E. Harris, *Phys. Today* **50**, 36 (July 1997).
8. M. D. Lukin, S. F. Yelin, and M. Fleischhauer, *Phys. Rev. Lett.* **84**, 4232 (2000).
9. M. Fleischhauer and M. D. Lukin, *Phys. Rev. Lett.* **84**, 5094 (2000).
10. M. G. Raymer, I. A. Walmsley, J. Mostowski, and B. Sobolewska, *Phys. Rev. A* **32**, 332 (1985); M. G. Raymer and I. A. Walmsley, in *Progress in Optics*, ed. E. Wolf, North-Holland, Amsterdam, Vol. **28**, p. 181 (1996)
11. An analogous process is superradiance triggered by vacuum fluctuations in the electromagnetic field, see for example M. Gross and S. Haroche, *Phys. Rep.* **93**, 301 (1982).
12. D. F. Walls and G. J. Milburn, *Quantum Optics*, Springer-Verlag, Berlin, 1994.
13. B. E. A. Saleh and M. C. Teich, *Fundamentals of photonics*, John Wiley and Sons, Inc., New York, 1991.
14. M. D. Lukin, P. R. Hemmer, M. Löffler, and M. O. Scully, *Phys. Rev. Lett.* **81**, 2675 (1998).
15. A. André *et al.*, to be published.
16. O. Aytür and P. Kumar, *Phys. Rev. Lett.* **65**, 1551 (1990).
17. P. C. D. Hobbs, *Building electro-optical systems: making it all work*, John Wiley and Sons, Inc., New York, 2000; M. B. Gray, D. A. Shaddock, C. C. Harb, and H. A. Bachor, *Rev. Sci. Instr.* **69**, 3755 (1998).